

Asymmetry effects on the phases of RKKY-coupled two-impurity Kondo systems

Krzysztof P. Wójcik^{1,2,3,*} and Johann Kroha^{3,†}

¹*Institute of Physics, Maria Curie-Skłodowska University, 20-031 Lublin, Poland*

²*Institute of Molecular Physics, Polish Academy of Sciences, Smoluchowskiego 17, 60-179 Poznań, Poland*

³*Physikalisches Institut, Universität Bonn, Nussallee 12, D-53115 Bonn, Germany*

(Dated: September 26, 2022)

In a related work [arXiv:2106.07519] we have shown that in the two-impurity Anderson (2iA) model with two hosts coupled by spin exchange in the most symmetric case there are either two phase transitions or none. The phases comprise the conventional Kondo and RKKY regimes and a novel one, interpreted as a Kondo-stabilized, metallic quantum spin liquid (QSL). Here we analyze how various types of asymmetry affect this picture. We demonstrate that the transitions are robust against the coupling and particle-hole asymmetries, provided charge transfer is forbidden. This holds true despite the scattering phase shift at each impurity taking non-universal values. Finally, for an extended model including charge transfer between the hosts and a small Coulomb interaction at the host sites directly coupled to impurities, we show that the presence of charge transfer changes the phase transitions into crossovers. Provided the inter-host hopping is sufficiently small, this leads to qualitatively the same physics at non-zero temperature. The relevance of this model for rare-earth atoms in a metallic host is discussed and potential experimental setups for observing our findings are proposed.

I. INTRODUCTION

Heavy fermion (HF) materials have been studied for many years, yet their rich phase diagrams still elude precise understanding [1, 2]. In particular, already in 1977 Doniach proposed a scenario [3] for HF magnetic phase transitions to be qualitatively captured by the competition of the local Kondo screening of individual impurities and the long-range conduction-band-mediated, indirect spin exchange between distinct impurities, the RKKY interaction [4–6]. This local perspective gained particular interest after it has been shown that already in the case of two impurities it can trigger a quantum phase transition (QPT) [7–9], related to two-channel Kondo physics [10, 11]. Since then, two-impurity or dimer systems have become a test ground for many concepts concerning HF properties [12–16]. This strategy is further supported by the recent, successful dynamical mean-field theory (DMFT) mapping of a generic Kondo lattice onto self-consistent two-impurity problem [17].

Nevertheless, the significance of the Jones-Varma QPT for HF criticality is still debated for a number of reasons. (1) It relies on strong assumptions concerning, in particular, a special type of particle-hole (PH) symmetry, and the QPT is in general smeared into crossover in less symmetric cases [18–20]. In real materials PH symmetry is usually not present. Still, a properly tuned counter-term allows to restore the transition in the partly symmetric model [21]. The absence of charge transfer between the hosts suffices to observe the transition in theory for two impurities [19, 22], and self-consistency restores the stability of the transition within DMFT of the Kondo lattice

with anti-ferromagnetic order [17]. In experiments, even the presence of a small charge transfer seems to not suppress the two-impurity QPT [12].

(2) In a dense impurity lattice there may be too few electrons for complete screening of all the impurities independently, as suggested by Nozières’ exhaustion principle [23, 24] and proven recently for the periodic Anderson model [25]. This suggests a reinterpretation of the metallic HF system as composed of partially correlated impurities instead of individually Kondo-screened ones.

(3) It has been stressed that in many HF materials an important role is played by frustration [1, 26] which competes with ordering tendencies and may lead to exotic phases, including metallic QSLs [27–32], coexistence of the Kondo effect and QSL [33] or magnetic ordering of residual local magnetic moments [34–40]. This intensively researched field applies to materials possessing magnetic moments arranged into triangular or other frustrated lattices, but seems less related to cases lacking geometrical frustration, such as studied here.

(4) The Jones-Varma model neglects that the realistic RKKY interaction is conduction-electron mediated, but replaces it by a direct Heisenberg exchange between the impurities as an independent parameter. The resulting phase diagram is different from the 2iA model with an individual host for each impurity and a spin exchange between the two hosts [41]. Remarkably, there a QSL phase occurs even without geometrical frustration, but stabilized against a dimerized phase by the Kondo effect [41–43]. Most recently, the RKKY coupling is also considered as an indirect interaction in Ref. [44] for a Kondo necklace model, but there the lack of charge degrees of freedom excludes a QSL phase studied here.

In the present paper, we take Ref. [41] as a starting point and analyze how the results presented there depend on different types of asymmetry. In Sec. II we introduce the model, explaining different types of asymme-

* kpwojcik@ifmpan.poznan.pl

† kroha@th.physik.uni-bonn.de

try in Secs. II B-II D and the methodology in Sec. II E. The simplicity of the proposed two-impurity setup allows for a near-exact numerical solution, in particular without any type of mean-field treatment nor perturbative approximations. In Sec. III we give detailed definitions of all crossover scales relevant to the model, and elaborate on the role of interactions in the conduction band for the stability of the spin liquid phase. Sec. IV is devoted to the description of the results in different asymmetric cases. In particular, we show that the zero-temperature phase diagram obtained in Ref. [41] stays intact despite PH or Kondo coupling asymmetry. Then, in Sec. IV C, we show that the presence of charge transfer changes the QPTs into crossovers, such that soft-boundary regimes of similar properties replace the well-defined phases of the symmetric model. We conclude in Sec. V.

II. MODEL AND ITS SYMMETRIES

A. Fully symmetric case

The model consists of two impurities, each one coupled to a different host. The hosts are coupled by a spin exchange, as depicted schematically in Fig. 1(a). The Hamiltonian is based on the Anderson impurity model for each of the *channels*, where each host together with its corresponding impurity is referred to as a channel. Therefore, its symmetrical form reads

$$H = \sum_{\alpha\mathbf{k}\sigma} \varepsilon_{\alpha\mathbf{k}} \hat{c}_{\alpha\mathbf{k}\sigma}^\dagger \hat{c}_{\alpha\mathbf{k}\sigma} + \sum_{\alpha\mathbf{k}\sigma} V_\alpha (\hat{c}_{\alpha\mathbf{k}\sigma}^\dagger \hat{d}_{\alpha\sigma} + \text{h.c.}) + \sum_{\alpha\sigma} \varepsilon_\alpha \hat{n}_{\alpha\sigma} + U \sum_{\alpha} \hat{n}_{\alpha\uparrow} \hat{n}_{\alpha\downarrow} + J_Y \vec{s}_1 \vec{s}_2, \quad (1)$$

where $\hat{n}_{\alpha\sigma} = \hat{d}_{\alpha\sigma}^\dagger \hat{d}_{\alpha\sigma}$ is the number operator of spin- σ electrons on the impurity α ($\alpha \in \{1, 2\}$ and $\sigma \in \{\uparrow, \downarrow\}$), the conduction-band spin operator at the impurity site in channel α is defined as $\vec{s}_\alpha = \sum_{\mathbf{k}\mathbf{k}'} \hat{c}_{\alpha\mathbf{k}\sigma}^\dagger \vec{\sigma}_{\sigma\sigma'} \hat{c}_{\alpha\mathbf{k}'\sigma'}$, with $\vec{\sigma}$ the vector of Pauli matrices. $V_1 = V_2 \in \mathbb{R}$ determine the hybridization between the impurity and the host in respective channel. Finally, U denotes the Coulomb repulsion within the impurity orbitals, while J_Y is the inter-host spin-exchange coupling. J_Y with suppressed charge transport may possibly be created by large-spin molecules or a chain of magnetic atoms in between the two impurities, as in Ref. [22]. The impurity-host hybridization functions are $\Gamma_{\alpha\sigma}(\omega) = \pi \rho_{\alpha\sigma}(\omega) V_\alpha^2$, where $\rho_{\alpha\sigma}$ denotes the density of host states. We assume a constant, spin-independent and PH symmetric host density of states within the bandwidth D_α , $\rho_{\alpha\sigma}(\omega) \equiv N^{-1} \sum_{\mathbf{k}} \delta(\omega - \varepsilon_{\alpha\mathbf{k}\sigma}) \approx (2D_\alpha)^{-1}$ for $|\omega| \leq D_\alpha$ (N is the number of \mathbf{k} points in momentum space) and $\rho_{\alpha\sigma}(\omega) = 0$ for $|\omega| > D_\alpha$. We will comment on the case $D_1 \neq D_2$ when discussing channel asymmetry, see Sec. IV A, and assume $D_1 = D_2 = D$ otherwise. As long as $\rho_{\alpha\sigma}(\omega)$ is regular at the Fermi level, their energy dependence is expected to be unimportant at low temperatures [45].

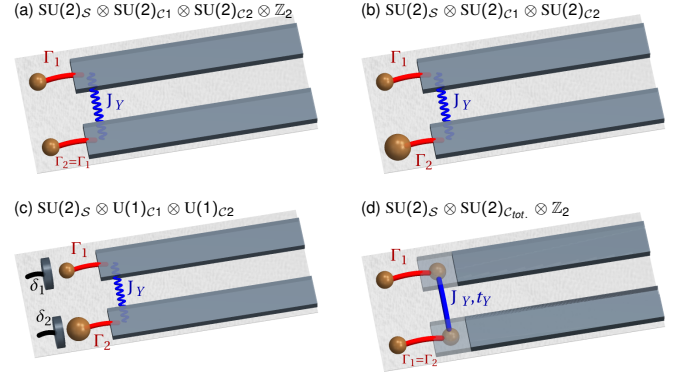


Figure 1. (a) Schematic illustration of the fully symmetric model of Ref. [41]. (b-d) Different types of asymmetric models considered in the present paper: (b) model with channel asymmetry, (c) model with PH asymmetry, (d) model with allowed inter-channel charge transfer.

Discussing the significance of (partial) spin polarization of the leads would be relevant for ferromagnetically correlated leads and require an additional study.

Setting the energy levels of the impurities at $\varepsilon_\alpha = -U/2$ ensures the full PH symmetry of the model, while independence of the Hamiltonian parameters of α guarantees channel symmetry. The symmetry of the model is then the same as the one studied originally by Jones and Varma [8]. The total symmetry of the model is a product of several subgroups, $SU(2)_S \otimes SU(2)_{C_1} \otimes SU(2)_{C_2} \otimes \mathbb{Z}_2$, described as follows. The first term corresponds to conventional total spin (denoted S) conservation in the absence of anisotropy. Furthermore, the electric charge is conserved in each of the channels separately, and in the presence of PH symmetry the conventional $U(1)_{C_\alpha}$ charge symmetries are lifted to an isospin $SU(2)_{C_\alpha}$, where the z -component of the isospin is the physical charge, and the isospin rising and lowering corresponds to PH transformations. Finally, the \mathbb{Z}_2 symmetry corresponds to the invariance of the Hamiltonian with respect to interchanging the channels.

Noteworthy, in the conventional 2iA model with a single host, the $SU(2)_{C_\alpha}$ charge symmetries do in general not appear for both channels of the effective NRG model separately [21]. The different types of asymmetry taken into consideration in the present paper are explained one by one in the following and examined for their influence on the phase diagram of the model in Sec. IV.

B. Channel asymmetry

Channel asymmetry appears when the hybridizations of impurities with their respective hosts differ between the channels, *i.e.* $\Gamma_1 \neq \Gamma_2$ as in Fig. 1(b), or $V_1 \neq V_2$ in Eq. (1). This, in turn, implies different Kondo couplings and different Kondo temperatures, T_{K1} and T_{K2} , characterizing the corresponding channels. Due to the

exponential dependence of $T_{K\alpha}$ on Γ_α , even a small difference in Γ_α renders large discrepancy of Kondo scales. Hence, the discussion of this asymmetry seems necessary for making a reliable connection to experimental reality. Technically, this means that the \mathbb{Z}_2 symmetry is broken, while all three $SU(2)$ symmetries remain intact.

C. Particle-hole asymmetry

The PH symmetry plays a special role in the context of the Jones-Varma two-impurity model. In fact, it has been recognized that only a special type of PH symmetry guarantees the existence of QPT which is otherwise turned into a crossover [18, 19]. However, it has subsequently been proven that the QPT is robust even in the absence of PH symmetry and destabilized only by charge transfer between the hosts [22, 46]. Moreover, the only marginally relevant perturbation around the QPT fixed point can be eliminated by an appropriate counter-term, such as additional inter-impurity hopping [21]. Therefore, it seems that the analysis cannot be complete without checking if the Kondo-RKKY transition and the QSL transition, reported in Ref. [41], share this characteristics. To this end, we set $\varepsilon_\alpha = -U/2 + \delta_\alpha$ in Eq. (1) and study the properties of the system for different detunings from the PH symmetry point δ_α , as schematically presented in Fig. 1(c). $\delta_\alpha \neq 0$ reduces the charge symmetry of channel α from $SU(2)$ to regular $U(1)$ charge conservation.

As a particular case, PH asymmetry includes the situation when individual channels are asymmetric, yet compensate each other to restore global (weak) PH symmetry, $\delta_1 = -\delta_2$ for $\Gamma_1 = \Gamma_2$. However, as shown below, also in the more general case of independent detuning of the energy levels of each impurity the transitions stay intact.

D. Charge transfer

We also analyze the situation of allowed charge transfer between the hosts. By this we mean adding a hopping term t_Y to Eq. (1), that is, considering the Hamiltonian

$$H_{\text{asym}} = H + U_{\text{cb}} \sum_{\alpha} \hat{c}_{\alpha\uparrow}^{\dagger} \hat{c}_{\alpha\uparrow} \hat{c}_{\alpha\downarrow}^{\dagger} \hat{c}_{\alpha\downarrow} + t_Y \sum_{\sigma} (\hat{c}_{1\sigma}^{\dagger} \hat{c}_{2\sigma} + \text{h.c.}), \quad (2)$$

where $\hat{c}_{\alpha\sigma} = \sum_{\mathbf{k}} \hat{c}_{\alpha\mathbf{k}\sigma}$ denotes the conduction-electron operator with spin σ at the site of the impurity α . Note, that in this case the two hosts sites are, in fact, interacting, as schematically depicted in Fig. 1(d).

Introducing $U_{\text{cb}} > 0$ is well motivated in particular in the case when the impurities are f or d -electron adatoms, such as Ce or Co, on a metal surface. Then, the f or d -electron carries the Kondo impurity spin and simultaneously hybridizes with the s -electrons of the same

impurity atom, where the local Coulomb interaction is much weaker, $U_{\text{cb}} < U$. In turn, the s -orbital is coupled to the itinerant host electrons [12]. We note in passing that a similar model with $U_{\text{cb}} \neq 0$ would emerge in DMFT for an anti-ferromagnetic phase of the Kondo-Hubbard model relevant for manganites, even though the Kondo coupling would need to be replaced by ferromagnetic Hund's exchange there [47, 48].

Since asymmetries different from charge transfer terms are irrelevant (see above), below we will restrict ourselves to the PH- and channel-symmetric case for the sake of simplicity. Nevertheless, the results are expected to apply to the general case.

E. Methods

The model is solved by the numerical renormalization group (NRG) procedure [45, 49]. Our implementation is based on the open-access code Ref. [50], which uses the basis set of all discarded states [51] to construct the full density matrix of the system [52]. This allows to calculate static expectation values for any temperature T and compute arbitrary spectral functions in a sum-rule-conserving framework, directly in their Lehmann representation. In all NRG calculations we use the NRG discretization parameter $\Lambda = 2.5$. At each NRG step we keep all states with (rescaled) energy E_j below a cut-off value E_{cut} , where E_{cut} is chosen within the range $6.5 < E_{\text{cut}} < 7.0$ (in units of the iteration scale) such that the energy difference between the last kept and the first discarded state is greater than 0.001. For all calculations we choose Hamiltonian parameter values (as given in the following) such that the intrinsic energy scales are well separated and the different regimes can be clearly identified.

To avoid ambiguities introduced by artificial broadening of the spectral functions, instead of studying the spectral densities directly, we will use the impurity conductance G and the conduction-band conductance g , defined as

$$G_{\alpha}(T) = \sum_{\sigma} \int \mathcal{A}_{\alpha}(\omega) \left(-\frac{\partial f_T(\omega)}{\partial \omega} \right) d\omega, \quad (3)$$

$$g_{\alpha}(T) = \sum_{\sigma} \int \mathcal{B}_{\alpha}(\omega) \left(-\frac{\partial f_T(\omega)}{\partial \omega} \right) d\omega, \quad (4)$$

where $\mathcal{A}_{\alpha} = -\Gamma_{\alpha} \text{Im} \langle \langle \hat{d}_{\alpha\sigma}; \hat{d}_{\alpha\sigma}^{\dagger} \rangle \rangle^{\text{ret}}(\omega)$ is the normalized spectral density at the impurity α , which is independent of σ due to $SU(2)$ spin symmetry, and similarly $\mathcal{B}_{\alpha} = -2D_{\alpha} \text{Im} \langle \langle \hat{c}_{\alpha\sigma}; \hat{c}_{\alpha\sigma}^{\dagger} \rangle \rangle^{\text{ret}}(\omega)$. $f_T(\omega)$ denotes the Fermi-Dirac distribution function at temperature T and $\langle \langle \dots \rangle \rangle^{\text{ret}}$ the retarded fermionic Green function in frequency space. With the definitions Eq. (3) and (4), the conductance measured with an STM tip coupled to impurity α (conduction band site in direct vicinity of impurity α) is proportional to G_{α} (g_{α}), respectively. Since the actual conductance would depend on the coupling strength

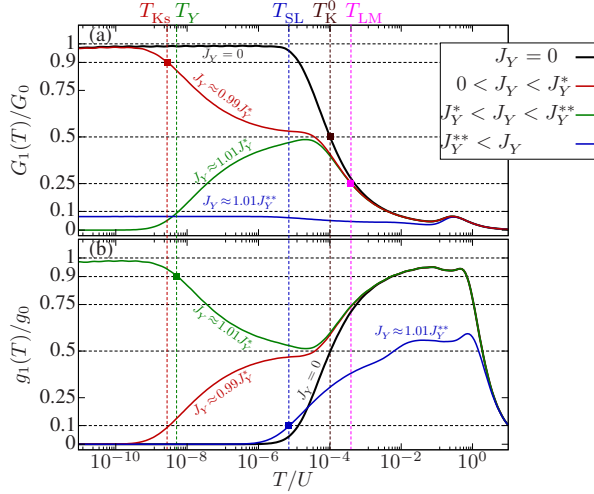


Figure 2. (a) Impurity conductance G_1 and (b) conduction-band conductance g_1 as functions of temperature T (note the logarithmic scale) for a symmetric model with $\Gamma_1 = \Gamma_2 = 0.0488U$ ($T_{K1}^0 = T_{K2}^0 \approx 10^{-4}U$), and a few values of J_Y , representative for various regimes (the actual values are $J_Y/D \in \{0, 0.105, 0.107, 1.5\}$). Other parameters: $D = 2U$, $\Lambda = 2.5$, $6.5 < E_{\text{cut}} < 7$.

between the STM and the impurity (host), we normalize it by its maximal value G_0 (g_0), corresponding to resonant transport conditions.

III. CROSSOVER TEMPERATURES AND PROPERTIES OF THE SPIN-LIQUID PHASE

In this section we corroborate and extend the results of Ref. [41] in that we provide a detailed explanation of the relevant energy scales, an analysis of the fixed point spectra in the respective phases of the model, and a more extensive discussion of the Heisenberg transition in the conduction band. We consider the symmetric model of Eq. (1), with $D_1 = D_2 = D = 2U$ and $\Gamma_1 = \Gamma_2 = \Gamma = 0.0488U$, which results in a single-impurity ($J_Y = 0$) Kondo temperature of $T_{K\alpha}^0 \approx 10^{-4}U$. It exhibits two QPTs when J_Y is increased from 0 to $J_Y \gg D$ [41]. These results will then be used as a reference for the asymmetry analysis in Sec. IV.

A. Crossover temperatures and Kondo destruction

We first introduce a number of crossover scales that characterize the NRG flow of the fully symmetric system from the weak-coupling local-moment fixed point at high energy to the low-energy fixed points describing the various ground-state phases of our system, the Kondo, the RKKY, and the QSL phase, respectively, depending on the value of J_Y . This flow can be observed in the T dependence of the G_1 and g_1 as shown for the symmetric case ($G_2 = G_1$ and $g_2 = g_1$) in Fig. 2 (a), (b). Above

the conduction bandwidth, $T > D = 2U$, G_1 and g_1 approach zero due to the absence of spectral density. G_1 features a bump at $T \approx U/2$ where excitations to empty and doubly occupied impurity states are thermally accessible. Correspondingly, g_1 has a dip at $T \approx U/2$ due to a Fano-like depletion of conduction spectral density. It is evident from the figure that in the general case ($J_Y \neq 0$), for $T < U/2$ the temperature dependence is governed by two scales. In the local-moment regime (decoupled impurity spins) we have $G_1/G_0 \approx 0$ and $g_1/g_0 \approx 1$, so that we can define the scale below which the system deviates from the local-moment regime as the temperature T_{LM} where $G_1(T_{\text{LM}})/G_0 = 0.25$ and $g_1(T_{\text{LM}})/g_0 = 0.75$, see Fig. 2 (a), (b).

The low- T scales can be read off from Fig. 2 as follows. The Kondo regime is characterized by $G_1(0)/G_0 = 1$, $g_1(0)/g_0 = 0$, while in the RKKY regime $G_1(0)/G_0 = 0$, $g_1(0)/g_0 = 1$. Consequently, we can define the scale on which the Kondo fixed point is approached ($0 < J_Y < J_Y^*$) as the strong-coupling Kondo temperature T_{Ks} where $G_1(T_{\text{Ks}})/G_0 = 0.9$ and $g_1(T_{\text{Ks}})/g_0 = 0.1$ (red curves), while the approach to the RKKY fixed point ($J_Y^* < J_Y < J_Y^{**}$) is characterized by the scale T_Y with $G_1(T_Y)/G_0 = 0.1$, $g_1(T_Y)/g_0 = 0.9$ (green curves). The approach to the QSL fixed point ($J_Y > J_Y^{**}$) is more difficult to characterize as the impurity conductance G_1 assumes non-universal low- T values in this case [blue curve in Fig. 2 (a)], while $g_1(0)/g_0 = 0$. Therefore, we define the QSL scale T_{SL} as the temperature where $g_1(T_{\text{SL}}) = 0.1$ [blue curve in Fig. 2 (b)].

We note that in the limit of a single Anderson impurity ($J_Y = 0$) the strong and weak coupling scales T_{Ks} and T_{LM} become proportional to each other (not shown), signaling the universality of the single-impurity Anderson model. We find that the Kondo fixed point is approached at low T once $G(T)/G_0$ exceeds the separating value of $1/2$ and $g_1(T)/g_0$ drops below $1/2$, see Fig. 2. Within the Kondo regime ($0 < J_Y < J_Y^*$) we can, thus, characterize the flow by a single Kondo scale $T_K(J_Y)$ with $G_0[T_K(J_Y)] = 1/2$. For non-zero RKKY-like coupling $J_Y \neq 0$, $T_K(J_Y)$ is suppressed below its single-impurity value $T_K(J_Y = 0) = T_K^0$ and ceases to exist beyond the critical coupling J_Y^* . We find $T_K(J_Y^*) = T_K^0/e$, where $e = 2.718\dots$ is Euler's constant, in agreement with the analytic result of Ref. [53] (see Fig. 3 of Ref. [41]). Thus, $T_K(J_Y)$ is a crossover scale which can be identified with a renormalized, single-impurity Kondo temperature which remains finite at the transition. By contrast, the strong-coupling scale T_{Ks} drops to 0 quadratically at the Kondo-to-RKKY QPT as a function of J_Y , in agreement with the Kondo destruction hypothesis [28, 54–56], here confirmed for the 2-impurity case. Similarly, $T_Y(J_Y)$ vanishes quadratically at the QSL transition, see insets of Fig. 3 (c) of Ref. [41]. When channel asymmetry is included, a significant channel dependence of all the scales leads to qualitatively different regimes at $T > 0$ which we analyze in Sec. IV A.

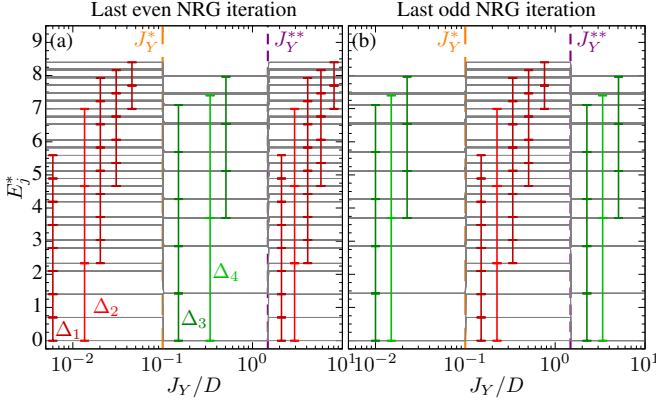


Figure 3. Fixed point many-body spectra (1000 multiplets with lowest energy) at (a) last even and (b) last odd NRG iteration, for parameters as in Fig. 2 with $T = 10^{-7}T_K^0 = 10^{-11}U$, as functions of J_Y . The QPTs are indicated with dashed vertical lines. All the many-body excitation energies can be composed of only 4 single-particle excitation energies Δ_1 – Δ_4 (see text for details).

B. Fixed point spectra and Fermi-liquid character

Further insight into the structure of the Kondo, RKKY, and QSL phases can be gained from the fixed-point spectra in these phases, *i.e.*, the spectra of the (scaled) renormalized Hamiltonian to which the system converges for a large number of NRG iterations. As is well known, these spectra differ for even or odd number of NRG iterations, because in each iteration one site is added to a Wilson chain and the total electron number (per channel) increases by one, so that the many-body ground state is alternately a spin singlet or a Kramers doublet [25, 45, 49].

The fixed-point spectra of the symmetric model, Eq. (1), are displayed in Fig. 3 as function of J_Y for the last even and last odd iteration, clearly showing the two phase transitions as discontinuities at $J_Y = J_Y^*$ and J_Y^{**} , respectively. We see that all three stable phases are of Fermi liquid (FL) nature, (but not the critical fixed points marking the transitions). This can be recognized from the fact, that the eigenenergies E_j^* of the truncated fixed-point Hamiltonian up to about $j_{\max} = 1000$ multiplets can be constructed as a linear combination of only two level spacings, namely, for even iterations $E_j^* = n\Delta_1 + m\Delta_2$ in the Kondo phase ($J_Y < J_Y^*$) and $E_j^* = n\Delta_3 + m\Delta_4$ in the RKKY phase ($J_Y^* < J_Y < J_Y^{**}$) with integer n, m . This is indicated in Fig. 3 (a) by the vertical rulers. It means that the many-body states with energies E_j^* consist of multiple independent excitations of the same energies Δ_i , the quasiparticle excitations characteristic of a FL. For the chosen $\Lambda = 2.5$, we have $\Delta_1 = 0.699$, $\Delta_2 = 2.332$ and $\Delta_3 = 1.422$, $\Delta_4 = 3.698$.

In fact, in the Kondo phase the fixed-point spectrum is identical to that of the free conduction system ($\Gamma = 0$, $J_Y = 0$, not shown) which is a FL by definition. It

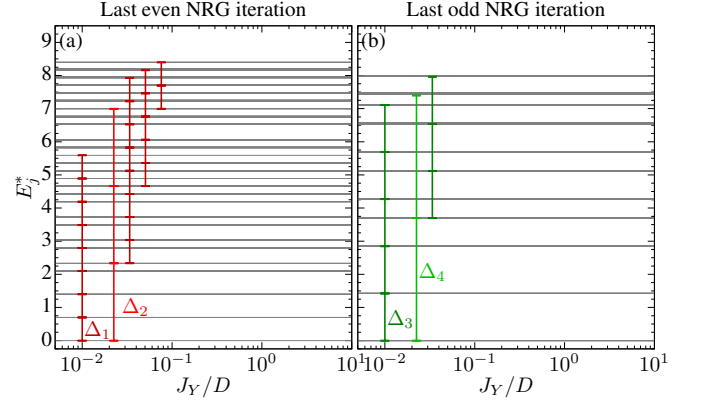


Figure 4. Like Fig. 3, except for $\Gamma = 0.103U$ corresponding to $T_K^0 \approx 10^{-2}U$, and with $T = 10^{-7}T_K^0 = 10^{-9}U$. There are no QPTs in this case. Excitation energies Δ_1 – Δ_4 are the same as in Fig. 3.

results from the fact that effectively one conduction electron from each channel is used to form the Kondo singlet with the respective impurity and the remaining conduction electrons are free particles with an impurity scattering phase shift of $\varphi = \pi/2$ at the fixed point. In the RKKY phase, the fixed-point spectrum is the same as in the case of free particles. Here, the Kondo screening is absent, thus, the impurity scattering phase shift $\varphi = 0$. However, because of the Heisenberg interaction J_Y within the conduction electron system, the relevant quasiparticles are superpositions of free Bloch electrons, still forming FL excitations. Finally, it is interesting to see in Fig. 3 that the fixed-point spectra of the Kondo and the RKKY phases are interchanged when one considers the odd- instead of even-iteration spectra. This simply stems from the fact that in the Kondo phase one conduction electron is effectively removed from the system by the Kondo screening as compared to the RKKY phase, and the same is true when one considers the system in the $(N-1)$ st (odd) iteration instead of the N th (even) iteration (see above).

Coming now to the QSL phase ($J_Y > J_Y^{**}$), it is striking in Fig. 3 that the QSL fixed-point spectrum is identical to the Kondo fixed-point spectrum. This means, in particular, that the QSL is also a FL. However, it should be stressed at this point that the identical fixed point spectrum does not mean that the two phases are the same. The eigenstates are different compositions of the original degrees of freedom, in particular leading to a spreading of the phase shift into the interacting part of the conduction band and consequently non-universal values of impurity spectral density. This can be interpreted as non-universal fractionalization of the FL quasiparticles into conduction-band and impurity parts. The former are responsible for the partial Kondo-screening of the impurities. The latter give rise to interimpurity spin correlations of the QSL (see also Sec. III C). Nevertheless, the identical spectra indicate the possibility that

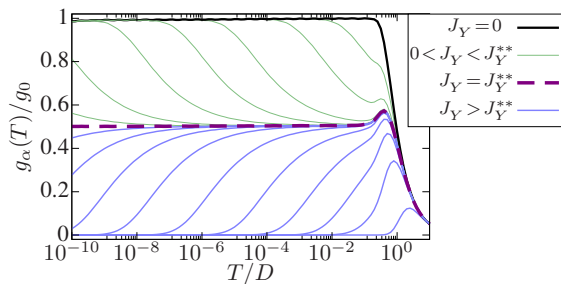


Figure 5. Conduction band conductance g_α in a special case of $\Gamma_1 = \Gamma_2 = 0$, as a function of temperature, for different J_Y in the range indicated in the legend. Other parameters as in Fig. 2.

the two phases can be continuously connected by circumventing the $T = 0$ phase transitions in parameter space. This scenario is indeed realized for strong enough Kondo coupling Γ , measured by T_K^0 , as is shown by the fixed-point spectrum in Fig. 4 for $T_K^0 \approx 10^{-2}U$ and by the general phase diagram in Fig. 2 (b) of Ref. [41]. The Kondo-QSL crossover corresponds to a continuous change of the proportions between the two parts of the quasi-particles driven by increasing J_Y . In this case the Kondo fraction of them starts melting around $J_Y \sim D$ and the inter-channel fraction dominates completely only in the $J_Y \rightarrow \infty$ limit.

C. Significance of the interaction in the band

In conventional impurity models, the case of vanishing Kondo coupling is trivially a Fermi liquid (plus the decoupled impurities). However in the case of the Hamiltonian given by Eq. (1), even for $\Gamma_1 = \Gamma_2 = \Gamma = 0$ there is an interaction term proportional to J_Y , acting within the conduction band. Therefore, let us consider now the case $\Gamma = 0$. After NRG mapping onto the Wilson chains, this model is very similar to the Jones-Varma model [8] except that, instead of the localized spins, J_Y couples two sites strongly hybridizing with the bath and possessing charge as well as spin degrees of freedom, since the Coulomb repulsion is absent. Despite these differences, an analogue of the Jones-Varma transition is still present and actually corresponds to the spin-liquid transition at $J_Y = J_Y^{**} \approx 1.5D$. It is driven by the spin exchange destabilizing the Bloch electrons when overcoming the corresponding bandwidth. This is illustrated in Fig. 5, showing the conductance g_α as a function of T . However, in the absence of impurities, the non-universal character of the phase for $J_Y > J_Y^{**}$ is lost, for the impurity fraction of the quasiparticles cannot exist then (see previous section). Instead, a soft-gapped FL emerges, fully characterized by a density of states featuring universal $\mathcal{B}(\omega) \sim \omega^2$ behavior.

The lack of conduction band electrons near the Fermi level comes from the fact that this state may also be seen

as an analogue of a Kondo state, where each of the two conduction bands plays the role of a spin-screening channel for the other. This binds the electrons from the Fermi level into spin singlets, as it does in the Kondo effect. The important difference is that, unlike the Kondo coupling, J_Y does not flow under RG transformations, thus, a critical value of J_Y must be exceeded for this phase to form. On the other hand, it should be noted that in the absence of interactions within the conduction band, coupling the impurity to a host with a static, not dynamically generated density of states proportional to ω^2 , does not lead to the screening of the impurity spin, even in the presence of strong Kondo coupling [57–59]. Hence, it is the competition between both dynamical effects, the tendency to form the interchannel screening induced by J_Y and the Kondo effect induced by non-zero Γ , that generates the frustration stabilizing the QSL phase in the presence of Kondo impurities. In this Kondo-stabilized QSL the impurity spectral density acquires a nonuniversal value at $\omega = 0$. The screening of each impurity by the respective conduction band and the interimpurity local spin compensation both contribute to the non-universal ground state correlations. The scattering phase shift of the free part of conduction band electrons gets spread between the impurities and the interacting part of the conduction band. For sufficiently strong Γ , decreasing J_Y then leads to a continuous crossover to the Kondo state, with each impurity screened by the respective conduction band. The above observation points to the expectation that, in order to capture a possible QSL of the type discussed here in Kondo lattice systems, it is essential to treat both effects dynamically, the Kondo screening and the spin correlations within the conduction band. The latter is not performed in single-site DMFT [60].

IV. ASYMMETRY

In the present section we analyze each type of asymmetry, case by case, showing that the general scenario obtained for the symmetric case survives at $T = 0$ as long as there is no charge transfer. Moreover, even in the presence of the latter many features of the symmetric model can be identified in extended regimes, corresponding to the sharp phases of the symmetric model. However, channel asymmetry splits the Kondo scale into two different values for each channel, $T_K^0 \rightarrow T_{K1}^0, T_{K2}^0$, and a large difference between the two will create space for qualitatively new behavior at $T > 0$.

A. Results for channel asymmetry

1. General picture

As the first type of asymmetry we study the channel asymmetry. Let us start by inspecting the flow diagram for $\Gamma_2 = \Gamma_1/2$, which is presented in Fig. 6. First of all,

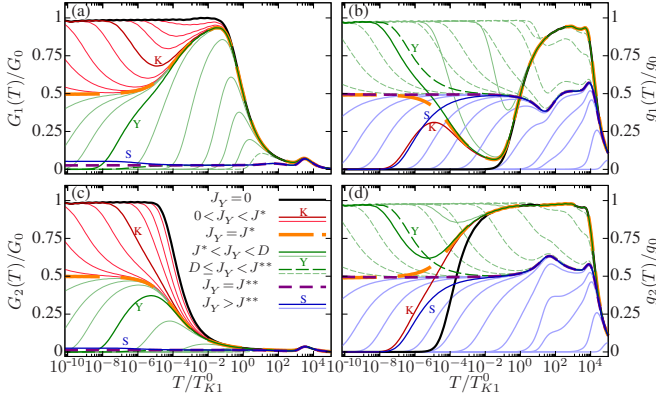


Figure 6. The flow diagrams of the impurity conductances (a) G_1 and (c) G_2 as well as the conduction-band conductances (b) g_1 , and (d) g_2 , in presence of channel asymmetry induced by a difference in the Kondo couplings, $\Gamma_2 = 0.5 \Gamma_1 = 0.0244U$. Other parameters: $D = 2U$, $\Lambda = 2.5$, $6.5 < E_{\text{cut}} < 7$. Representative flow curves towards the Kondo, RKKY, and SQL fixed points are marked with K, Y, and S, respectively.

we clearly see that reducing Γ_2 by a factor of 2 drives the corresponding Kondo temperature T_{K2}^0 down by almost 4 orders of magnitude, a manifestation of its exponential dependence on the coupling strength, cf. Fig. 6 (c). This separation of energy scales facilitates analyzing the regime $T_{K2} \ll T \ll T_{K1}$ by NRG, see below. For smaller asymmetry, this intermediate regime is realized at higher temperatures. For $T < \min(T_{K1}, T_{K2})$ all the properties of the symmetric model [41] are recovered. In particular, the impurity conductances exhibit universal values: $G_1(T=0) = G_2(T=0) = G_0$ in the Kondo regime ($J_Y < J_Y^*$) and $G_1(0) = G_2(0) = 0$ in the RKKY phase ($J_Y^* < J_Y < J_Y^{**}$). The two phases are separated by a Jones-Varma QPT [8], *i.e.*, the unstable QPT fixed point at $J_Y = J_Y^*$ where $G_1(0) = G_2(0) = G_0/2$. Further increase of J_Y drives the spin-liquid QPT [41] at $J_Y = J_Y^{**} \approx 1.5D$, where the values of $G_1(0)$ and $G_2(0)$ become non-universal.

For a Fermi liquid in the presence of PH symmetry, the only two possible values of scattering phase shift from an impurity are 0 or $\pi/2$ [19, 61]. However, the J_Y term in Eq. (1) acting between the hosts does not correspond to a single-particle dispersion, but introduces interactions into the conduction band. For this reason, G_α , $\alpha = 1, 2$, does not have to assume a universal value at $T \rightarrow 0$. Nevertheless, as this is the only interacting term in the leads, the remaining parts of the electrodes (*i.e.* each entire electrode α excluding the state on which J_Y directly acts) are still a FL, and the phase-shift argument is valid for $g_\alpha(0)$. Therefore, $g_\alpha(0)$ always assumes universal values 0 or g_0 , except for the critical points at $J_Y = J_Y^*$ and $J_Y = J_Y^{**}$, where non-Fermi-liquid critical fixed points allow for $g_1(0) = g_2(0) = g_0/2$. Thus, together with $G_\alpha(0)$, the values of $g_\alpha(0)$ characterize all the phases uniquely, in exactly the same way as for the channel-symmetric case [41].

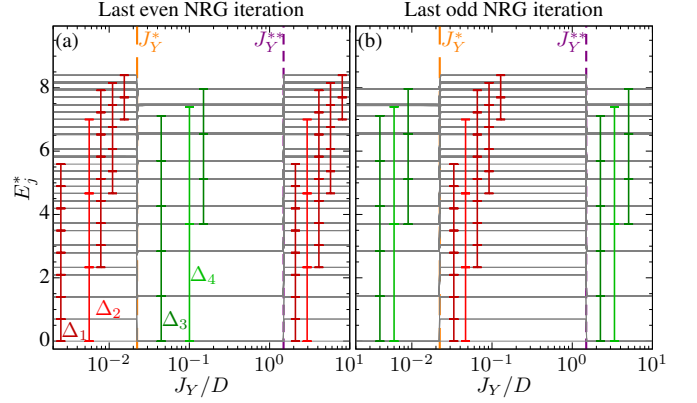


Figure 7. Fixed-point spectra at the (a) last even and (b) last odd NRG iteration for parameters as in Fig. 6 with $T = 10^{-7}T_{K1}^0 = 10^{-11}U$ as functions of J_Y . The QPT points are indicated by vertical, dashed lines.

While at $T = 0$ the regimes of the channel-asymmetric model are the same as in the symmetric one, the situation changes at $T > 0$. For $T_{K2} < T < T_{K1}$, the second impurity is still in the local-moment regime, such that neither the Kondo effect nor the RKKY interaction are significant there. Meanwhile, the first impurity is already screened by its host. In such conditions T_{K1}^0 is almost not affected by J_Y , as seen in Fig. 6 (a). Only at lower $T \approx T_{K2}^0$, $G_1(T)$ drops from a value close to G_0 , characteristic of the Kondo regime, towards the unstable QPT fixed-point value $G_0/2$. Upon further decreasing $T \rightarrow 0$, in the Kondo phase ($J_Y < J_Y^*$) $G_1(T)$ returns to the unitary value $G_1(0) = G_0$ and in the RKKY phase ($J_Y^* < J_Y < J_Y^{**}$) it further drops to $G_1(0) = 0$. In this way, the stronger-coupled impurity approaches the Kondo regime twice: once at $T \lesssim T_{K1}$, and then again at $T < T_{Ks2}$. In between, at $T \sim T_{K2}$ the second impurity leaves the local-moment regime, and its flow toward the

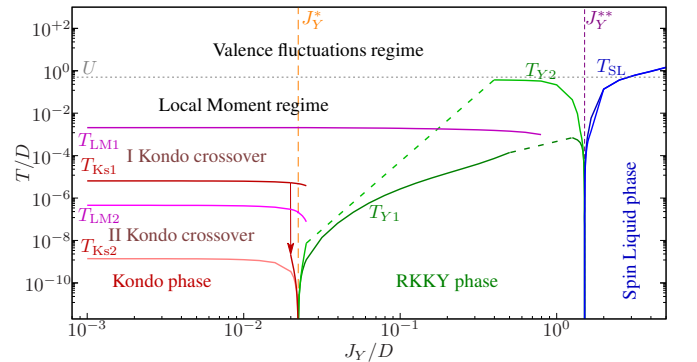


Figure 8. Phase diagram obtained from the NRG flow of Fig. 6. The ambiguity of T_{Ks1} (indicated by the vertical arrow next to the J_Y^* line) is caused by the fact that the Kondo regime is approached twice. T_{Y1} and T_{Y2} are not well defined far from the transitions and represented as dashed, straight lines. In the QSL phase, $T_{SL1} = T_{SL2} = T_{SL}$.

Kondo regime affects the screening in the first channel via the RKKY interaction, which becomes relevant in this temperature range. Hence, for the first, stronger-coupled impurity, T_{Ks1} is not unique then, and only one of these two strong-coupling Kondo scales vanishes at the Jones-Varma transition as in the symmetric case, while the other one does not, cf. Fig. 6 (a). On the other hand, for the second impurity, T_{Ks2} is more efficiently suppressed to zero than in the symmetric case, cf. Fig. 6 (c). The host conductances g_α behave as can be expected on the basis of the symmetric case. They reveal all the characteristic energy scales in their temperature dependencies. As can be seen in Figs. 6, $g_\alpha(T)/g_0 \approx 1 - G_\alpha(T)/G_0$ except for the QSL phase, where g_α vanishes despite a small, non-universal G_α . The fixed-point spectra for the parameter values as in Fig. 6 are shown in Fig. 7, confirming that the Fermi liquid nature of the three different phases is preserved in the channel-asymmetric case, see the discussion in Sec. III B.

Summarizing the asymmetric NRG flow of Fig. 6, the phase diagram in the J_Y - T plane is presented in Fig. 8. Note that the scales $T_{LM\alpha}$, $\alpha = 1, 2$, persist across the Jones-Varma transition and the strong-coupling scale of the weaker-coupled impurity, T_{Ks2} vanishes, as expected from the symmetric case. However, the low-energy scale of the stronger-coupled impurity, T_{Ks1} , splits into two values, $T'_{Ks2} > T_{Ks2}$ where the larger one remains finite across the QPT. This means that the expected scaling behavior near the QPT will exist only for $T < T'_K$, which should be experimentally observable in asymmetric setups. By contrast, both $T_{Y\alpha}$ scales vanish at the QSL transition.

2. Dependence on asymmetries Γ_2/Γ_1 and D_2/D_1

Let us now inspect G_α and g_α as functions of J_Y at a cryogenic but non-zero temperature $T = 10^{-11}U$, see Fig. 9. For $\Gamma_2 = 2\Gamma_1$ there are two phase transitions similar to the symmetric case ($\Gamma_2 = \Gamma_1$), as already discussed in the context of Figs. 6 and 8. With decreasing Γ_2/Γ_1 at fixed $\Gamma_1 = 0.0488U$ the Jones-Varma phase boundary J_Y^* shifts towards smaller values. We can estimate this decrease analytically in the following way. In the presence of asymmetric Kondo couplings there exist two different single-impurity Kondo scales, see also Fig. 6. For a PH-symmetric Anderson impurity model ($\varepsilon_\alpha = U/2$), they are approximately given by [62]

$$T_{K\alpha}^0 = \sqrt{U\Gamma_\alpha} e^{-\pi U/8\Gamma_\alpha}, \quad \alpha = 1, 2. \quad (5)$$

The RKKY coupling can be calculated perturbatively as

$$Y \simeq (\rho_1 J_{K1})(\rho_2 J_{K2}) J_Y, \quad (6)$$

with the Kondo spin-exchange coupling $\rho_\alpha J_{K\alpha} = 4\rho_\alpha V_\alpha^2/U = 4\Gamma_\alpha/\pi U$. Generalizing the Doniach criterion for RKKY-induced Kondo breakdown [3] to channel asymmetry, the state with two individually Kondo

screened impurities is expected to terminate when Y reaches a critical strength which is roughly given by the smaller one of the two Kondo scales. This is confirmed by the NRG flow in Fig. 6, where it is the smaller one of the two scales that determines which fixed point is reached at the lowest energy, with some modification of $T_{K\alpha}$ by the inter-channel coupling J_Y . Combining this criterion with Eqs. (5), (6) we obtain the critical inter-channel coupling for the asymmetric Jones-Varma transition ($\Gamma_2 < \Gamma_1$),

$$J_Y^* \simeq \frac{(\pi U)^2}{4\Gamma_1} \sqrt{\frac{U}{\Gamma_2}} e^{-\pi U/8\Gamma_2}, \quad (7)$$

which is exponentially suppressed with Γ_2/U . When T_{K2} becomes smaller than the temperature T of the system, the transition gets smeared as seen in Fig. 9 for $\Gamma_2/\Gamma_1 = 0.25$.

Note that the QSL transition persists even for the smallest Γ_2/Γ values, since its characteristic energy scale is fixed at $J_Y^* \approx 1.5D \gg T$ [41]. On the other hand, when the asymmetry Γ_2/Γ_1 exceeds a certain threshold, J_Y^* exceeds J_Y^* , *i.e.*, the intermediate RKKY phase vanishes, and the two QPTs merge to a single Kondo-to-QSL crossover [41], as seen in Fig. 9 for $\Gamma/\Gamma_1 = 4$.

To summarize this section, the $\Gamma_2 \neq \Gamma_1$ case is qualitatively the same as the symmetric case at $T = 0$, as long as the effective scale for Kondo breakdown does not exceed the threshold value for changing the 2-QPTs scenario to the no-QPT scenario. However, at elevated T a novel regime appears, when one of the impurities is practically decoupled. The RKKY interaction and the Kondo effect on the more weakly coupled impurity are not relevant there, while the QSL phase remains robust, unless one of the impurities is completely detached. The extreme asymmetric limit of decoupling one impurity is subtle and requires further study beyond the scope of the present article. We further find that asymmetry in the bandwidths, $D_2/D_1 \neq 1$, (not shown) causes effects similar to the coupling asymmetry. It leads to different Kondo scales $T_{K\alpha}$ and crossover scales $T_{Y\alpha}$ etc., but does not drive qualitatively new phenomena.

B. Results for particle-hole asymmetry

We now focus on the PH asymmetry as defined in Sec. II C, still in the absence of inter-channel charge transfer. We consider first the channel-symmetric case, $\delta_1 = \delta_2 = \delta$, so that $G_1 = G_2$ and analogous for all other physical quantities.

Fig. 10 shows that the two QPTs, visible as discontinuities of the conductances G_1 and g_1 as functions of J_Y near zero temperature, $T = 11^{-11}U$, are robust against PH symmetry breaking, just as the Jones-Varma transition is in the case of direct inter-impurity spin exchange, see Ref. [22]. With increasing PH asymmetry δ the first, Jones-Varma-like QPT shifts from $J_Y^* \approx 0.1D$ to larger critical values J_Y^* , while the second QPT at $J_Y^* \approx 1.5D$

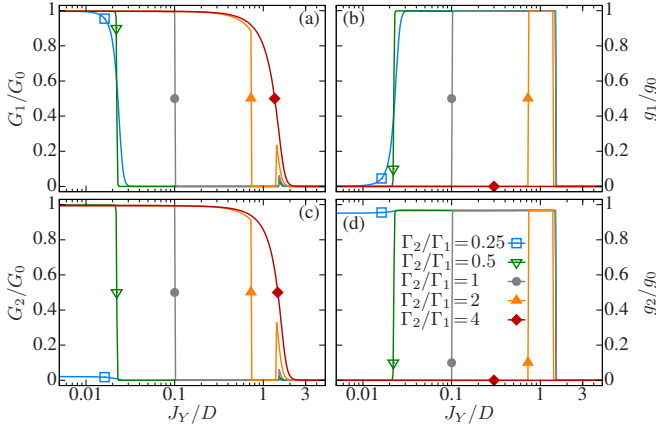


Figure 9. The conductances G_α (left panels) and g_α (right panels), $\alpha = 1, 2$, as functions of J_Y for $T = 10^{-11}U$ and various ratios of the Kondo couplings Γ_2/Γ_1 for fixed $\Gamma_1 = 0.0488U$. Other parameters are as in Fig. 6.

is independent of δ , until both QPTs merge into a single crossover for $\delta \gtrsim U/3$ [red curves in Fig. 10 (a), (b)]. This behavior can be understood in the following way. According to the Doniach criterion [3] the Kondo breakdown occurs when the effective RKKY interaction Y exceeds the single-impurity Kondo scale T_K^0 , where $Y \sim [\rho J_K(\delta)]^2 J_Y$ and $J_K(\delta) = (\Gamma/\pi)[U/(U^2/4 - \delta^2)]$ from a Schrieffer-Wolff transformation [62, 63] of the Hamiltonian Eq. (1). PH-asymmetry thus leads to a squared exponential increase of the Kondo scale,

$$T_K^0(\delta) = T_K^0(0) e^{\pi\delta^2/(2\Gamma U)}, \quad (8)$$

and, therefore, to an increase of the critical $J_Y^*(\delta)$ of the Jones-Varma transition, independent of the sign of δ . The merging of the two QPTs to a single crossover with increasing $T_K(0)$, i.e., the vanishing of the RKKY phase at a critical point $T_{K\max}^0$ was explained for the PH-symmetric case in Sec. III and observed in the phase diagram of Ref. [41], Fig. 2. Here, it is an experimentally relevant observation that one can switch between the single-crossover and the double-QPT scenarios by tuning the PH asymmetry, *e.g.*, by gating the impurity levels.

From Fig. 10 we see that $G_\alpha/G_0 \approx 1$ and $g_\alpha \approx 0$ for

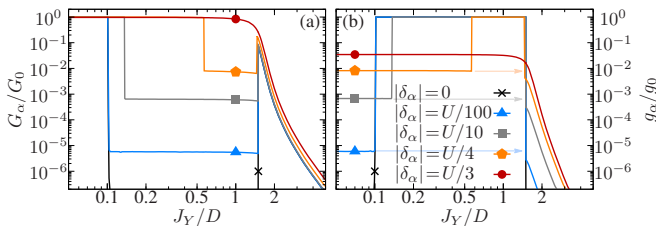


Figure 10. $G_1 = G_2$ and $g_1 = g_2$ as functions of J_Y for $T_K^0 = 10^{-7}U$, $T = 10^{-11}U$, $\Lambda = 2.5$, and PH asymmetry $|\delta_1| = |\delta_2|$. Other parameters are as in Fig. 2. The results do not depend on the sign of δ_α .

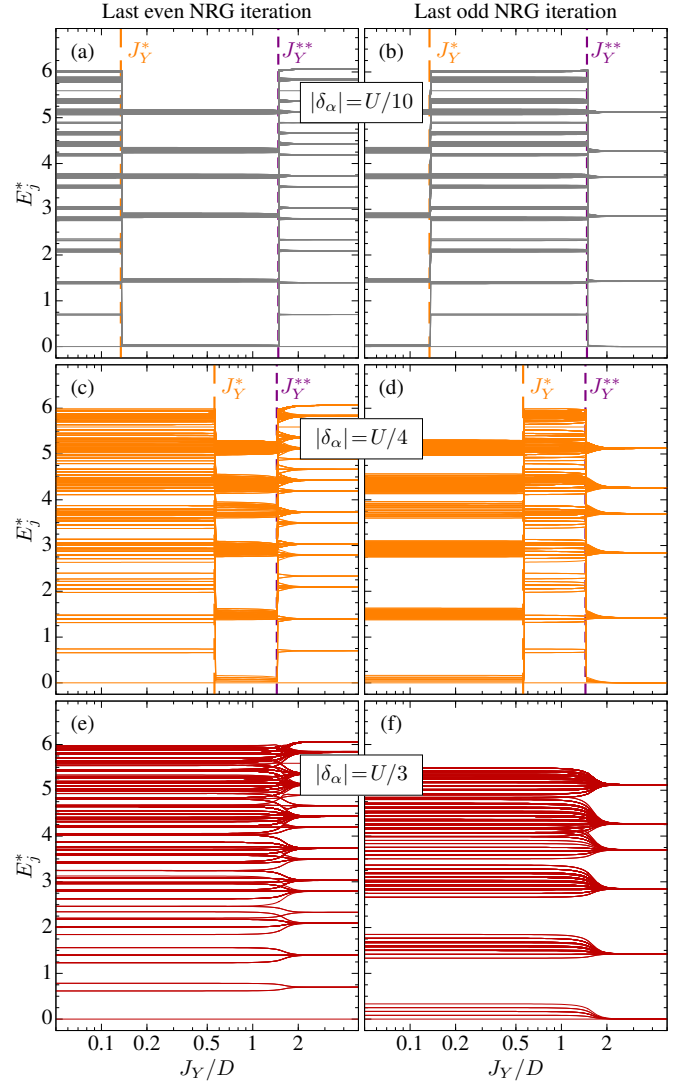


Figure 11. Fixed point spectra (lowest 1000 states) for PH asymmetry, $\delta_\alpha \neq 0$. Parameters and a color code are the same as in Fig. 10, with (a-b) $|\delta_\alpha| = U/10$, (c-d) $|\delta_\alpha| = U/4$, (e-f) $|\delta_\alpha| = U/3$. Note that the $\delta_\alpha = 0$ case is presented in Fig. 3.

$J_Y < J_Y^*$. However, with $|\delta_\alpha| > 0$ small non-universality appears, characteristic of asymmetric Anderson model [64], well visible as small $g_\alpha > 0$ values, even in the $T \rightarrow 0$ limit. Similarly, in the RKKY phase ($J_Y^* < J_Y < J_Y^{**}$) G_α takes nonzero values. These are signatures of nonuniversal scattering phase shifts of the band electrons in both regimes. The persistence of true QPTs even in this nonuniversal situation is a special feature of the two-host model Eq. (1), designed to describe an effective RKKY interaction without charge transfer. It is in stark contrast to the conventional single-host 2-impurity model, where the QPT can be restored by a fine-tuned counter-term only if the phase shifts from the two impurities compensate each other [21].

The above properties are corroborated by the fixed-point spectra shown in Fig. 11. The persisting QPTs

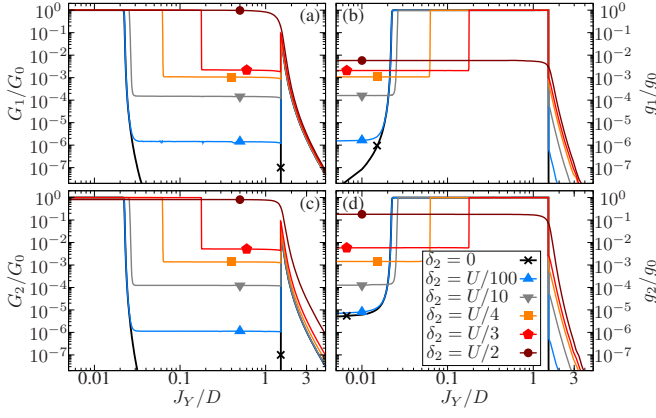


Figure 12. Conductances as functions of J_Y for $T_2 = T_1 = 0.0488U$ and $\delta_2 = 2\delta_1$. Other parameters as in Fig. 10.

are clearly visible as discontinuities of the spectra below the crossover threshold, $T_K^0 < T_{K\max}^0$, Fig. 11 (a)–(d). However, the spectra are no longer universal as in the fully symmetric case. Instead, the low-lying multiplets get split, a manifestation that each δ_1, δ_2 renders a marginally relevant perturbation to the PH-symmetric fixed point, extending the latter into a surface of fixed points, analogous to the line of fixed points in the case of a single impurity Anderson model [64]. Above the threshold, $T_K^0 > T_{K\max}^0$, the spectra show a crossover from the Kondo to the QSL regime, as expected [Fig. 11 (e), (f)].

Finally, in Fig. 12 we show the results for the channel-asymmetric case in addition to PH asymmetry, $\delta_\alpha \neq 0$. As seen in the figure, the effects of both types of asymmetry just “add up”. PH asymmetry induces non-universality, while channel asymmetry is relevant mainly at elevated temperatures and does not lead to qualitatively new features. Imposing $|\delta_1| \neq |\delta_2|$ does not induce qualitative changes, albeit the level of deviation of G_α from universality is substantially increased in the channel with larger δ_α .

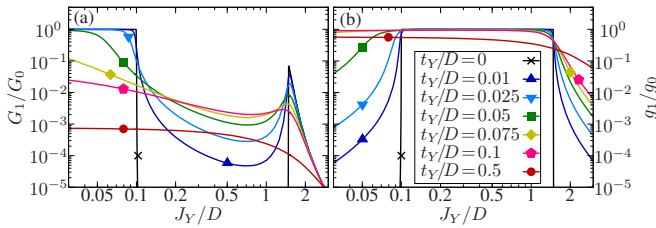


Figure 13. $T = 0$ conductances $G_1(0)$ and $g_1(0)$ as functions of J_Y for different inter-site hoppings t_Y , and $U_{cb} = U/100$. Other parameters as in Fig. 10 with $\delta_\alpha = 0$, except $\Lambda = 3$ and $5.5 < E_{\text{cut}} < 6$.

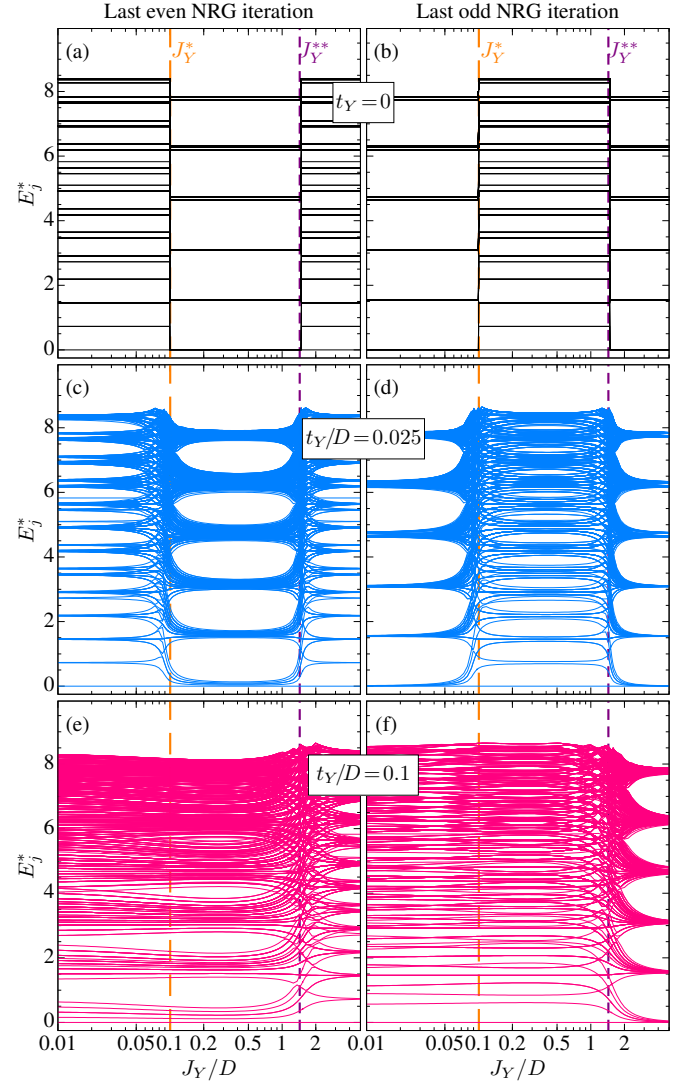


Figure 14. The fixed point spectra (lowest 1000 states) for (a-b) $t_Y = 0$, (c-d) $t_Y = 0.025D$ and $t_Y/D = 0.1$ (e-f). Vertical lines indicate the positions of QPTs at $t_Y = 0$. Parameters as in Fig. 13. Note that due to $\Lambda = 3$ the energy levels cannot be directly compared to Figs. 3, 11 etc.

C. Results in the presence of charge transfer

In this section we address the case with charge transfer allowed between the channels by $t_Y \neq 0$, as introduced in Sec. IID, and all other parameters symmetric. The most important results concerning charge transfer are presented in Fig. 13, where $G_1 = G_2$ and $g_1 = g_2$ are plotted as functions of J_Y . The NRG parameters used there, $\Lambda = 3$ and $5.5 < E_{\text{cut}} < 6$, are slightly modified in comparison to earlier figures, to reduce the numerical effort increased by lifting the intra-host $U(1)$ symmetries.

Without charge transfer, the Jones-Varma and the QSL QPTs exist at $J_Y = J_Y^* \approx 0.1D$, in agreement with the Doniach critical value of the RKKY coupling $Y^* \simeq [4\Gamma/(\pi\rho U)]^2 J_Y^* \approx T_K^0$, and at $J_Y = J_Y^{**} \approx 1.5D$,

corresponding to the characteristic quasiparticle energies in the Kondo and the RKKY phase, respectively [41]. For $t_Y \neq 0$, both QPTs get smeared into a crossover [18, 19], although t_Y also generates a contribution to the RKKY coupling. One can see from the logarithmic J_Y scale in Fig. 13 that for both crossovers and fixed t_Y , the crossover width scales roughly with the respective critical value, J_Y^* or J_Y^{**} . Noteworthy, t_Y destroys the universality features in both, the Kondo and the RKKY regimes by introducing a marginally relevant perturbation around the respective fixed points. Consequently, G_1 (g_1) does not reach unity in the Kondo (RKKY) regime, and does not drop to 0 in the RKKY (Kondo) regime. This loss of universality is further illustrated by the fixed point spectra in Fig. 14, where the levels, which are degenerate for $t_Y = 0$ (a-b), are split for $t_Y \neq 0$ (c-f), in addition to the smearing of the QPTs.

The smearing of the QPTs raises the question about their experimental observability in the presence of charge transfer. For the QSL transition, the inter-host magnetic coupling must reach $J_Y \gtrsim 1.5 D$. This seems possible in low-bandwidth systems, especially in magic-angle, twisted bilayer graphene [65, 66], doped with Kondo impurities and with an additional magnetic exchange J_Y between the hosts. However, magnetic exchange is usually accompanied by charge transfer. In Fig. 13 the crossovers are still well pronounced up to $t_Y/J_{Yc} \approx 0.1$, where $J_{Yc} = J_Y^* \approx 0.1 D$ for the Jones-Varma and $J_{Yc} = J_Y^{**} \approx 1.5 D$ for the QSL transition, but are washed out for larger t_Y/J_{Yc} values. This indicates that the QSL transition/crossover allows for significantly larger absolute values of charge transfer to be observed than the Jones-Varma transition. The narrow width of the QSL crossover for up to $t_Y \lesssim 0.05 D$ (see Fig. 13) gives rise to the expectation that this crossover should be well observable in two-impurity tunneling setups [12] or by reducing charge transfer by superexchange coupling of the hosts.

More important, however, would be the existence of a Kondo stabilized QSL in HF lattice systems. There, the metallic hosts of our model are represented by a single band with equal hopping matrix elements t between all neighboring sites. Charge transfer between lattice sites is, therefore, an integral part of the band. A recent DMFT study of the Anderson lattice with antiferromagnetic order competing with the Kondo effect [17] mapped such a lattice on a two-impurity model, where DMFT self-consistency restored the Jones-Varma-like QPT, even though charge transfer was present in the effective two-impurity model. This is similar to the restoration of the QPT by a fine-tuned counter-term as in Ref. [21], with the difference that the DMFT self-consistency (antiferromagnetic order) tunes the system to cancel the marginally relevant charge transfer operator, which otherwise would destabilize the transition. However, the study of Ref. [21] did not include genuine magnetic interactions within the conduction electron system as represented by the Heisenberg term J_Y in our

model, Eq. (1), which is instrumental in stabilizing the QSL phase. We, therefore, expect that in HF materials a QSL phase may be stabilized by strong, antiferromagnetic correlations within the conduction band (distinct from the Kondo-induced correlations), as they are generated, *e.g.*, near a spin-density-wave instability.

V. CONCLUSION

We have analyzed the influence of various types of asymmetry on a generic 2-impurity, 2-host Anderson system in the Kondo limit. We found that, as long as there is no charge transfer between the two screening channels, the results of the symmetric case apply qualitatively at sufficiently low temperatures. In particular, generically the system exhibits two QPTs. The Jones-Varma QPT occurs at a critical value J_Y^* when the inter-host spin exchange J_Y drives the RKKY coupling Y to overcome the effective Kondo scale of the system $T_K(J_Y)$, destroying Kondo quasi-particles. The second QPT is found for J_Y exceeding the critical value J_Y^{**} , close to the conduction bandwidth D . In the case of sufficiently strong Kondo couplings, J_Y^* may exceed J_Y^{**} , so that both QPTs merge to a single crossover.

If the Kondo couplings are not equal, two separate Kondo scales, T_{K1}^0 , T_{K2}^0 , appear in the NRG flow (each corresponding to one channel), and the position of the Jones-Varma QPT is roughly determined by the smaller one of the two Kondo scales. A novel regime appears in an elevated temperature range defined by $T_{K2} < T < T_{K1}$ when the Kondo scales of the two impurities are sufficiently different. In this interesting regime, at $J_Y \ll J_Y^{**}$, the system behaves as if the weaker-coupled impurity were detached. However, the QSL phase transition is robust, unless one of the impurities gets completely detached. Even PH asymmetry by independently gating the impurity levels does not lead to smearing of the QPTs. Instead, only the spectral densities acquire nonuniversal values. A similar behavior is expected for PH-asymmetric hosts. In line with Ref. [22], this gives hope for the experimental realization of the transitions in quantum-dot nanostructures.

We expect that a quantum spin liquid of the metallic type discussed here may be stabilized in heavy-fermion systems, near a spin-density wave instability of the conduction band, where strong antiferromagnetic correlations within the conduction band compete with Kondo screening of the localized moments, analogous to the inter-host spin coupling in the present two-impurity model.

ACKNOWLEDGMENTS

Stimulating discussions with Frithjof Anders, Fabian Eickhoff, Andreas Gleis, Mohsen Hafez-Torbati, and Kacper Wrzeński are gratefully acknowledged. This

project was financially supported by the Deutsche Forschungsgemeinschaft (DFG, German Research Foundation) under Germany's Excellence Strategy – Cluster of Excellence *Matter and Light for Quantum Computing*, ML4Q (390534769), and through the DFG Collaborative

Research Center CRC 185 OSCAR (277625399). K.P.W. acknowledges funding by the Alexander von Humboldt Foundation and support from the Polish National Science Centre through grant no. 2018/29/B/ST3/00937.

-
- [1] P. Coleman and A. H. Nevidomskyy, Frustration and the Kondo Effect in Heavy Fermion Materials, *J. Low Temp. Phys.* **161**, 182 (2010).
 - [2] S. Kirchner, S. Paschen, Q. Chen, S. Wirth, D. Feng, J. D. Thompson, and Q. Si, Colloquium: Heavy-electron quantum criticality and single-particle spectroscopy, *Rev. Mod. Phys.* **92**, 011002 (2020).
 - [3] S. Doniach, The Kondo lattice and weak antiferromagnetism, *Physica B+C* **91**, 231 (1977).
 - [4] M. A. Ruderman and C. Kittel, Indirect Exchange Coupling of Nuclear Magnetic Moments by Conduction Electrons, *Phys. Rev.* **96**, 99 (1954).
 - [5] T. Kasuya, A Theory of Metallic Ferro- and Antiferromagnetism on Zener's Model, *Prog. Theor. Phys.* **16**, 45 (1956).
 - [6] K. Yosida, Magnetic Properties of Cu-Mn Alloys, *Phys. Rev.* **106**, 893 (1957).
 - [7] B. A. Jones and C. M. Varma, Study of two magnetic impurities in a Fermi gas, *Phys. Rev. Lett.* **58**, 843 (1987).
 - [8] B. A. Jones, C. M. Varma, and J. W. Wilkins, Low-Temperature Properties of the Two-Impurity Kondo Hamiltonian, *Phys. Rev. Lett.* **61**, 125 (1988).
 - [9] B. A. Jones and C. M. Varma, Critical point in the solution of the two magnetic impurity problem, *Phys. Rev. B* **40**, 324 (1989).
 - [10] J. Gan, Mapping the Critical Point of the Two-Impurity Kondo Model to a Two-Channel Problem, *Phys. Rev. Lett.* **74**, 2583 (1995).
 - [11] A. K. Mitchell, E. Sela, and D. E. Logan, Two-Channel Kondo Physics in Two-Impurity Kondo Models, *Phys. Rev. Lett.* **108**, 086405 (2012).
 - [12] J. Bork, Y.-h. Zhang, L. Diekhöner, L. Borda, P. Simon, J. Kroha, P. Wahl, and K. Kern, A tunable two-impurity Kondo system in an atomic point contact, *Nat. Phys.* **7**, 901 (2011).
 - [13] A. Bayat, H. Johannesson, S. Bose, and P. Sodano, An order parameter for impurity systems at quantum criticality, *Nat. Commun.* **5**, 1 (2014).
 - [14] H. Prüser, P. E. Dargel, M. Bouhassoune, R. G. Ulbrich, T. Pruschke, S. Lounis, and M. Wenderoth, Interplay between the Kondo effect and the Ruderman-Kittel-Kasuya-Yosida interaction, *Nat. Commun.* **5**, 1 (2014).
 - [15] A. Spinelli, M. Gerrits, R. Toskovic, B. Bryant, M. Ternes, and A. F. Otte, Exploring the phase diagram of the two-impurity Kondo problem, *Nat. Commun.* **6**, 1 (2015).
 - [16] M. Moro-Lagares, R. Korytár, M. Piantek, R. Robles, N. Lorente, J. I. Pascual, M. R. Ibarra, and D. Serrate, Real space manifestations of coherent screening in atomic scale Kondo lattices, *Nat. Commun.* **10**, 1 (2019).
 - [17] A. Gleis, S.-S. Lee, A. Weichselbaum, G. Kotliar, and J. von Delft, To be published, (2022).
 - [18] R. M. Fye, Anomalous fixed point behavior” of two Kondo impurities: A reexamination, *Phys. Rev. Lett.* **72**, 916 (1994).
 - [19] I. Affleck, A. W. W. Ludwig, and B. A. Jones, Conformal-field-theory approach to the two-impurity Kondo problem: Comparison with numerical renormalization-group results, *Phys. Rev. B* **52**, 9528 (1995).
 - [20] J. B. Silva, W. L. C. Lima, W. C. Oliveira, J. L. N. Mello, L. N. Oliveira, and J. W. Wilkins, Particle-Hole Asymmetry in the Two-Impurity Kondo Model, *Phys. Rev. Lett.* **76**, 275 (1996).
 - [21] F. Eickhoff, B. Lechtenberg, and F. B. Anders, Effective low-energy description of the two-impurity Anderson model: RKKY interaction and quantum criticality, *Phys. Rev. B* **98**, 115103 (2018).
 - [22] G. Zaránd, C.-H. Chung, P. Simon, and M. Vojta, Quantum Criticality in a Double-Quantum-Dot System, *Phys. Rev. Lett.* **97**, 166802 (2006).
 - [23] P. Nozières, Impuretés magnétiques et effet Kondo, *Ann. Phys. Fr.* **10**, 19 (1985).
 - [24] Ph. Nozières, Some comments on Kondo lattices and the Mott transition, *Eur. Phys. J. B* **6**, 447 (1998).
 - [25] F. Eickhoff and F. B. Anders, Strongly correlated multi-impurity models: The crossover from a single-impurity problem to lattice models, *Phys. Rev. B* **102**, 205132 (2020).
 - [26] Q. Si, Quantum criticality and global phase diagram of magnetic heavy fermions, *Phys. Stat. Solidi (b)* **247**, 476 (2010).
 - [27] S. Nakatsuji, Y. Machida, Y. Maeno, T. Tayama, T. Sakakibara, J. v. Duijn, L. Balicas, J. N. Millican, R. T. Macaluso, and J. Y. Chan, Metallic Spin-Liquid Behavior of the Geometrically Frustrated Kondo Lattice $\text{Pr}_2\text{Ir}_2\text{O}_7$, *Phys. Rev. Lett.* **96**, 087204 (2006).
 - [28] S. Friedemann, T. Westerkamp, M. Brando, N. Oeschler, S. Wirth, P. Gegenwart, C. Krellner, C. Geibel, and F. Steglich, Detaching the antiferromagnetic quantum critical point from the Fermi-surface reconstruction in YbRh_2Si_2 , *Nat. Phys.* **5**, 465 (2009).
 - [29] S. Lucas, K. Grube, C.-L. Huang, A. Sakai, S. Wunderlich, E. L. Green, J. Wosnitza, V. Fritsch, P. Gegenwart, O. Stockert, and H. V. Löhneysen, Entropy Evolution in the Magnetic Phases of Partially Frustrated CePdAl , *Phys. Rev. Lett.* **118**, 107204 (2017).
 - [30] H. Zhao, J. Zhang, M. Lyu, S. Bachus, Y. Tokiwa, P. Gegenwart, S. Zhang, J. Cheng, Y.-f. Yang, G. Chen, Y. Isikawa, Q. Si, F. Steglich, and P. Sun, Quantum-critical phase from frustrated magnetism in a strongly correlated metal, *Nat. Phys.* **15**, 1261 (2019).
 - [31] M. Majumder, R. Gupta, H. Luetkens, R. Khasanov, O. Stockert, P. Gegenwart, and V. Fritsch, Spin-liquid signatures in the quantum critical regime of pressurized CePdAl , *Phys. Rev. B* **105**, L180402 (2022).
 - [32] R. Tripathi, D. T. Adroja, C. Ritter, S. Sharma, C. Yang, A. D. Hillier, M. M. Koza, F. Demmel, A. Sundare-

- san, S. Langridge, W. Higemoto, T. U. Ito, A. M. Strydom, G. B. G. Stenning, A. Bhattacharyya, D. Keen, H. C. Walker, R. S. Perry, F. Pratt, Q. Si, and T. Takabatake, Quantum critical spin-liquid-like behavior in $S = 1/2$ quasikagome lattice CeRh1-xPdxSn investigated using muon spin relaxation and neutron scattering, *arXiv* [10.48550/arXiv.2208.03148](https://arxiv.org/abs/10.48550/arXiv.2208.03148) (2022), [2208.03148](https://arxiv.org/abs/2208.03148).
- [33] H. Nobukane, Y. Tabata, T. Kurosawa, D. Sakabe, and S. Tanda, Coexistence of the Kondo effect and spin glass physics in Fe-doped NbS_2 , *J. Phys.: Condens. Matter* **32**, 165803 (2020).
- [34] C. Lacroix, B. Canals, and M. D. Núñez-Regueiro, Kondo Screening and Magnetic Ordering in Frustrated UNi_4B , *Phys. Rev. Lett.* **77**, 5126 (1996).
- [35] G.-B. Li, G.-M. Zhang, and L. Yu, Kondo screening coexisting with ferromagnetic order as a possible ground state for Kondo lattice systems, *Phys. Rev. B* **81**, 094420 (2010).
- [36] Y. Motome, K. Nakamikawa, Y. Yamaji, and M. Udagawa, Partial Kondo Screening in Frustrated Kondo Lattice Systems, *Phys. Rev. Lett.* **105**, 036403 (2010).
- [37] B. H. Bernhard and C. Lacroix, Coexistence of magnetic order and Kondo effect in the Kondo-Heisenberg model, *Phys. Rev. B* **92**, 094401 (2015).
- [38] T. Sato, F. F. Assaad, and T. Grover, Quantum Monte Carlo Simulation of Frustrated Kondo Lattice Models, *Phys. Rev. Lett.* **120**, 107201 (2018).
- [39] K. P. Wójcik, I. Weymann, and J. Kroha, Magnetic Kondo regimes in a frustrated half-filled trimer, *Phys. Rev. B* **102**, 045144 (2020).
- [40] M. Keßler and R. Eder, Magnetic phases of the triangular Kondo lattice, *Phys. Rev. B* **102**, 235125 (2020).
- [41] K. P. Wójcik and J. Kroha, Quantum spin liquid in an RKKY-coupled two-impurity Kondo system, *arXiv* [2106.07519v2](https://arxiv.org/abs/2106.07519v2) (2022).
- [42] P. Coleman and N. Andrei, Kondo-stabilised spin liquids and heavy fermion superconductivity, *J. Phys.: Condens. Matter* **1**, 4057 (1989).
- [43] N. Andrei and P. Coleman, Cooper Instability in the Presence of a Spin Liquid, *Phys. Rev. Lett.* **62**, 595 (1989).
- [44] M. Peschke, B. Ponsioen, and P. Corboz, Competing States in the Two-Dimensional Frustrated Kondo-Necklace Model, *arXiv:2209.04231* (2022).
- [45] K. G. Wilson, The renormalization group: Critical phenomena and the Kondo problem, *Rev. Mod. Phys.* **47**, 773 (1975).
- [46] E. Sela and I. Affleck, Resonant Pair Tunneling in Double Quantum Dots, *Phys. Rev. Lett.* **103**, 087204 (2009).
- [47] K. Held and D. Vollhardt, Electronic Correlations in Manganites, *Phys. Rev. Lett.* **84**, 5168 (2000).
- [48] M. Hafez-Torbati, D. Bossini, F. B. Anders, and G. S. Uhrig, Magnetic blue shift of Mott gaps enhanced by double exchange, *Phys. Rev. Res.* **3**, 043232 (2021).
- [49] R. Bulla, T. A. Costi, and T. Pruschke, Numerical renormalization group method for quantum impurity systems, *Rev. Mod. Phys.* **80**, 395 (2008).
- [50] O. Legeza, C. P. Moca, A. I. Toth, I. Weymann, and G. Zarand, Manual for the Flexible DM-NRG code, *arXiv:0809.3143* (2008). The code is available at <http://www.phy.bme.hu/~dmnrg/>.
- [51] F. B. Anders and A. Schiller, Real-Time Dynamics in Quantum-Impurity Systems: A Time-Dependent Numerical Renormalization-Group Approach, *Phys. Rev. Lett.* **95**, 196801 (2005).
- [52] A. Weichselbaum and J. von Delft, Sum-Rule Conserving Spectral Functions from the Numerical Renormalization Group, *Phys. Rev. Lett.* **99**, 076402 (2007).
- [53] A. Nejati, K. Ballmann, and J. Kroha, Kondo Destruction in RKKY-Coupled Kondo Lattice and Multi-Impurity Systems, *Phys. Rev. Lett.* **118**, 117204 (2017).
- [54] Q. Si, S. Rabello, K. Ingersent, and J. L. Smith, Locally critical quantum phase transitions in strongly correlated metals, *Nature* **413**, 804 (2001).
- [55] P. Coleman, C. Pépin, Q. Si, and R. Ramazashvili, How do Fermi liquids get heavy and die?, *J. Phys.: Condens. Matter* **13**, R723 (2001).
- [56] T. Senthil, M. Vojta, and S. Sachdev, Weak magnetism and non-Fermi liquids near heavy-fermion critical points, *Phys. Rev. B* **69**, 035111 (2004).
- [57] R. Bulla, T. Pruschke, and A. C. Hewson, Anderson impurity in pseudo-gap Fermi systems, *J. Phys.: Condens. Matter* **9**, 10463 (1997).
- [58] L. Fritz and M. Vojta, Phase transitions in the pseudogap Anderson and Kondo models: Critical dimensions, renormalization group, and local-moment criticality, *Phys. Rev. B* **70**, 214427 (2004).
- [59] T. Esat, B. Lechtenberg, T. Deilmann, C. Wagner, P. Krüger, R. Temirov, M. Rohlfing, F. B. Anders, and F. S. Tautz, A chemically driven quantum phase transition in a two-molecule Kondo system, *Nat. Phys.* **12**, 867 (2016).
- [60] A. Georges, G. Kotliar, W. Krauth, and M. J. Rozenberg, Dynamical mean-field theory of strongly correlated fermion systems and the limit of infinite dimensions, *Rev. Mod. Phys.* **68**, 13 (1996).
- [61] A. J. Millis, B. G. Kotliar, and B. A. Jones, In: Z. Tسانovic (ed.), *Many-Body Methods for Real Materials*, pp. 159–166 (Addison Wesley, Redwood City, CA, 1990).
- [62] F. D. M. Haldane, Scaling Theory of the Asymmetric Anderson Model, *Phys. Rev. Lett.* **40**, 416 (1978).
- [63] A. C. Hewson, *The Kondo problem to heavy fermions* (Cambridge University Press, Cambridge, 1997).
- [64] H. R. Krishna-murthy, J. W. Wilkins, and K. G. Wilson, Renormalization-group approach to the Anderson model of dilute magnetic alloys. II. Static properties for the asymmetric case, *Phys. Rev. B* **21**, 1044 (1980).
- [65] Y. Cao, V. Fatemi, A. Demir, S. Fang, S. L. Tomarken, J. Y. Luo, J. D. Sanchez-Yamagishi, K. Watanabe, T. Taniguchi, E. Kaxiras, R. C. Ashoori, and P. Jarillo-Herrero, Correlated insulator behaviour at half-filling in magic-angle graphene superlattices, *Nature* **556**, 80 (2018).
- [66] Y. Cao, V. Fatemi, S. Fang, K. Watanabe, T. Taniguchi, E. Kaxiras, and P. Jarillo-Herrero, Unconventional superconductivity in magic-angle graphene superlattices, *Nature* **556**, 43 (2018).